

A Mixed Integer Linear Programming Formulation for Unrestricted Wind Farm Layout Optimization

Ning Quan

Enterprise Systems Optimization Laboratory,
Department of Industrial and
Enterprise Systems Engineering,
University of Illinois at Urbana-Champaign,
Urbana, IL 61801
e-mail: nquan3@illinois.edu

Harrison M. Kim¹

Enterprise Systems Optimization Laboratory,
Department of Industrial and
Enterprise Systems Engineering,
University of Illinois at Urbana-Champaign,
Urbana, IL 61801
e-mail: hmkim@illinois.edu

This paper presents a novel mixed integer linear programming (MILP) formulation for finding the optimal layout of a fixed number of identical turbines that maximizes wind farm power generation. Previous MILP formulations with power maximizing objectives discretize the feasible space by using a grid of possible turbine locations. The proposed MILP formulation takes a different approach by allowing unrestricted placement of turbines, but treats wake cone overlap as a binary outcome. The rationale behind the proposed formulation is that the expansion of the feasible space for turbine placement in the proposed formulation would offset the disadvantage of using a lower fidelity binary wake cone overlap model. For small wind farms, the proposed formulation was able to produce superior layouts compared to a grid-based MILP formulation. [DOI: 10.1115/1.4033239]

1 Introduction

Wind power has emerged as one of the most promising renewable alternatives to fossil fuels in power generation [1,2]. Wind farms consisting of large horizontal axis turbines can be built at suitable sites both on or off-shore to harness wind energy for the power grid. Research into wind farm design has focused on answering three main questions—the size, number, and position of turbines in the wind farm. The answer to these three questions will determine the return on investment, reliability, and power generated by the wind farm. The reader can refer to Refs. [3] and [4] for a recent review of literature in wind farm design optimization.

It is assumed in this paper that the highly complex wind farm design problem is tackled using a multistage approach where planning questions such as turbine count, turbine type, and wind farm location are addressed prior to the last step of layout optimization. The focus of this paper is on the layout optimization problem where the goal is to find the layout of a predetermined number of similar turbines that maximizes wind farm power generation.

A primary concern in this class of problems is to minimize power loss due to wake-effects. Wind passing through a turbine's blades generates a wake cone—an area of turbulent, slower flowing air downstream of the turbine. When a turbine is placed within another turbine's wake cone, the power generated by the downstream turbine is reduced.

Previous works within this class of layout problems can be classified into discrete, continuous, or hybrid approaches depending on the feasible space for turbine placement. The discrete approach limits the positions of the turbines to a grid of possible locations. The continuous approach allows for unrestricted placement of turbines, and the final category is a combination of discrete and continuous approaches, hence the name “hybrid.”

Discrete, grid-based approaches have a smaller solution space than unrestricted continuous approaches, but it allows for MILP formulations [5,6] that can be solved to global optimality [7] if problem size is tractable. In cases when the problem size becomes too big, the grid-based formulation can be easily encoded into chromosomes for convenient application of genetic algorithms (GA) [8–10] to find good solutions.

In MILP formulations, the points in the grid can be seen as nodes in a graph, with edges between nodes representing wake effect interactions between the pair of grid points. The goal would then be to maximize or minimize the sum of edge costs depending on the nature of the problem. This framework also offers a convenient way of introducing additional concerns such as landowner participation [11], complex terrain [12–14], noise regulations [15], and nonconvex wind farm shapes into the basic power maximization formulation.

The continuous, unrestricted approach allows for all possible turbine layouts, but finding the global optimum out of all possible layouts is challenging task. The mathematical equations used to model turbine wake characteristics and wake interactions [16–18] are nonlinear and nonconvex/concave with respect to turbine locations which means the power generation objective function has multiple local minima. That is why many previous works in unrestricted layout optimization have used global search methods such as GAs [19,20], pattern search [21], ant colony algorithm [22], or particle swarm optimization [23].

The third, hybrid approach finds an initial turbine layout by adopting a regular lattice, or by using discrete, grid-based approaches mentioned above [24]. The hybrid approach then performs a local search of the continuous feasible space around the initial layout using gradient-based optimization methods [24–26] or random search methods such as particle swarm optimization [27].

The focus of this paper is on MILP formulations in wind farm layout optimization. Previous MILP formulations have all taken the discrete approach where turbines placement is limited to a grid of possibilities. The proposed MILP formulation offers an alternative to grid-based MILP formulations by showing it is possible to have unrestricted placement of turbines within a convex-shaped wind farm by treating wake cone overlap as a binary outcome.

MILP formulations such as the one proposed in this paper can be used to find good starting layouts for higher fidelity, continuous local search methods. Unlike grid-based formulations that are still dependent on the layout of the grid, the proposed MILP formulation with unrestricted placement of turbines is independent of any starting configuration.

Section 2 describes the proposed MILP formulation in detail, focusing in particular on the wake cone overlap detection constraints, objective function, and proximity constraints. Section 3 contains comparison results for a variety of scenarios between the proposed MILP formulation and a grid-based MILP formulation adapted from Ref. [6], and Sec. 4 concludes the paper.

¹Corresponding author.

Contributed by the Design Automation Committee of ASME for publication in the JOURNAL OF MECHANICAL DESIGN. Manuscript received October 6, 2015; final manuscript received March 22, 2016; published online April 20, 2016. Assoc. Editor: Carolyn Seepersad.

2 MILP Formulation

The proposed MILP formulation was designed with an emphasis on keeping the problem size in terms of number of binary variables as small as possible. One main theme in Secs. 2.1–2.4 is how redundant binary variables and constraints can be dropped from the proposed formulation without affecting solution quality.

There are three categories of constraints in the proposed MILP formulation—the first is used for detecting wake cone overlap for a given pair of turbines; the second category is used for enforcing minimum interturbine spacing; and the last category is used to enforce the boundaries of the wind farm, which is assumed to be a two-dimensional polyhedron. The first two categories along with the objective function are described in Secs. 2.1–2.4.

For the rest of the paper, let K and T denote the index set of wind directions and turbines, respectively. Each wind direction k is represented by a unit vector \mathbf{w}_k , and the location of turbine i is represented using the vector $\mathbf{x}_i \in \mathbb{R}^2$. Also, let $\mathbf{x}_{ij} \in \mathbb{R}^2$ be the vector from turbine i to turbine j ($\mathbf{x}_{ij} = \mathbf{x}_j - \mathbf{x}_i$).

2.1 Wake Cone Detection Constraints. It is assumed that the turbine disk is always orientated orthogonally to the oncoming wind direction. The wake behind the turbine disk takes the shape of a truncated cone (Fig. 1) with diameter given by Eq. (1), where D_0 is the diameter of the turbine disk, κ is the wake expansion coefficient, and d is the downstream distance

$$D(d) = D_0 + 2\kappa d \quad (1)$$

Wake cone membership in the formulation is treated as a binary outcome. A turbine is deemed to be inside an upstream turbine's wake cone if any part of its disk ($>0\%$) is inside the wake cone. This threshold can be changed to any value between 0% and 100% depending on the nature of the problem. For example, if space is very constrained, and layouts with zero overlaps are unlikely, then it might make sense to increase the overlap threshold to a higher value. For this work, the threshold is set to 0% for the rest of the paper.

Given any wind direction unit vector \mathbf{w}_k , let \mathbf{w}_k^l and \mathbf{w}_k^r be the left and right orthogonal unit vectors to \mathbf{w}_k as illustrated in Fig. 2. The left orthogonal unit vector is obtained by rotating \mathbf{w}_k clockwise by 90 deg, and the right orthogonal unit vector is obtained by rotating \mathbf{w}_k counterclockwise by 90 deg.

Any turbine pair identified using the notation (i, j) is shorthand for the query of whether turbine j is inside the wake cone generated by turbine i . Turbine j is deemed to be inside turbine i 's wake cone generated by wind direction \mathbf{w}_k if turbine j satisfies the following three conditions:

- Condition 1: The left edge of turbine j 's disk (\mathbf{x}_j^l), must be below the right wake cone edge of turbine i . This is equivalent to the expression $\mathbf{x}_{ij}^T \mathbf{w}_k^r - D_0/2 \leq D_0/2 + \kappa \mathbf{x}_{ij}^T \mathbf{w}_k$, where $D_0/2 + \kappa \mathbf{x}_{ij}^T \mathbf{w}_k$ is the radius of turbine i 's wake cone at a distance of $\mathbf{x}_{ij}^T \mathbf{w}_k$ along \mathbf{w}_k .
- Condition 2: The right edge of turbine j 's disk (\mathbf{x}_j^r), must be above the left wake cone edge of turbine i . This is equivalent to the expression $\mathbf{x}_{ij}^T \mathbf{w}_k^l - D_0/2 \leq D_0/2 + \kappa \mathbf{x}_{ij}^T \mathbf{w}_k$.
- Condition 3: $\mathbf{x}_{ij}^T \mathbf{w}_k \geq 0$ must be true, which is equivalent to the condition that turbine j must be located downstream of turbine i .

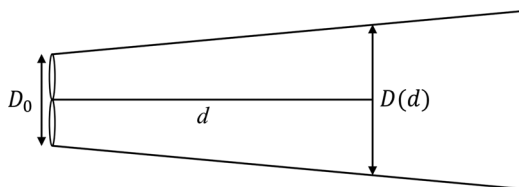


Fig. 1 Wake expansion

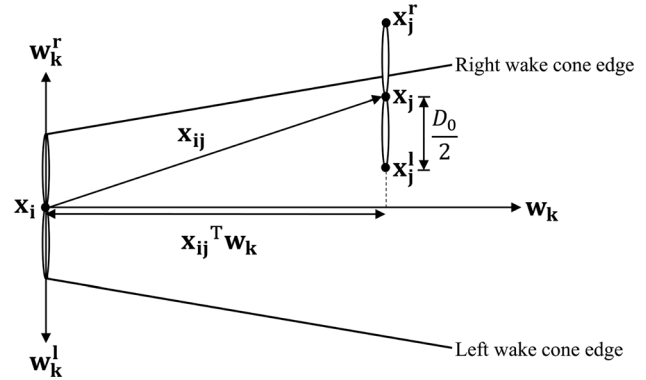


Fig. 2 Wake cone membership detection

Each of these conditions can be checked by introducing a binary indicator variable, and using linear “if-else” constraints. For example, given wind direction k and turbine pair (i, j) , let $z_{k,ij}^r$ be the indicator variable for condition 1. If turbine j satisfies condition 1 for turbine i 's wake cone generated by wind direction k , then $z_{k,ij}^r = 1$; otherwise, $z_{k,ij}^r = 0$. The value of $z_{k,ij}^r$ is determined using the two constraints shown in Eq. (2) where M_w is a constant set to the maximum value that the left-hand side of the constraint can take. The same procedure is followed for checking condition 2, whose indicator variable $z_{k,ij}^l$ and wake cone overlap constraints are shown in Eq. (3):

$$\begin{aligned} \mathbf{x}_{ij}^T \mathbf{w}_k^r - \frac{D_0}{2} - \left(\kappa \mathbf{x}_{ij}^T \mathbf{w}_k + \frac{D_0}{2} \right) &\leq M_w (1 - z_{k,ij}^r) \\ \kappa \mathbf{x}_{ij}^T \mathbf{w}_k + \frac{D_0}{2} - \left(\mathbf{x}_{ij}^T \mathbf{w}_k^r - \frac{D_0}{2} \right) &\leq M_w z_{k,ij}^r \end{aligned} \quad (2)$$

$$z_{k,ij}^r \in \{0, 1\}$$

$$\begin{aligned} \mathbf{x}_{ij}^T \mathbf{w}_k^l - \frac{D_0}{2} - \left(\kappa \mathbf{x}_{ij}^T \mathbf{w}_k + \frac{D_0}{2} \right) &\leq M_w (1 - z_{k,ij}^l) \\ \kappa \mathbf{x}_{ij}^T \mathbf{w}_k + \frac{D_0}{2} - \left(\mathbf{x}_{ij}^T \mathbf{w}_k^l - \frac{D_0}{2} \right) &\leq M_w z_{k,ij}^l \end{aligned} \quad (3)$$

$$z_{k,ij}^l \in \{0, 1\}$$

Condition 3 does not have to be checked explicitly if the turbines are ordered along a chosen axis and if the wind directions organized into sectors shown in Fig. 3. Ordering the turbines and organizing the wind directions into sectors also has the advantage of reducing the number of turbine pairs that have to be checked for wake cone overlaps. Section 2.1.1 describes this in greater detail.

2.1.1 Turbine Ordering and Wind Sectors. Ordering the turbines along a chosen axis can greatly reduce the feasible space of the MILP formulation without sacrificing any solution quality. Any corner of the wind farm can be chosen to be the origin of a two-dimensional coordinate system. The positive “horizontal” direction is chosen to be any of the wind directions, preferably one that runs along one of the principal sides of the wind farm. For simplicity, it is assumed that the horizontal wind direction has index “1.”

Turbines can then be ordered in ascending order along the horizontal axis according to their indexes as shown in Eq. (4), where $x_{i,\text{hor}}$ denotes the horizontal coordinate of turbine i .

$$x_{i,\text{hor}} < x_{j,\text{hor}} \quad \forall i, j \in T, \quad \forall i < j \quad (4)$$

Ordering the turbines along the horizontal axis also means that not all turbine pairs have to be checked for wake cone overlap in every wind direction. The wind directions are organized into 4

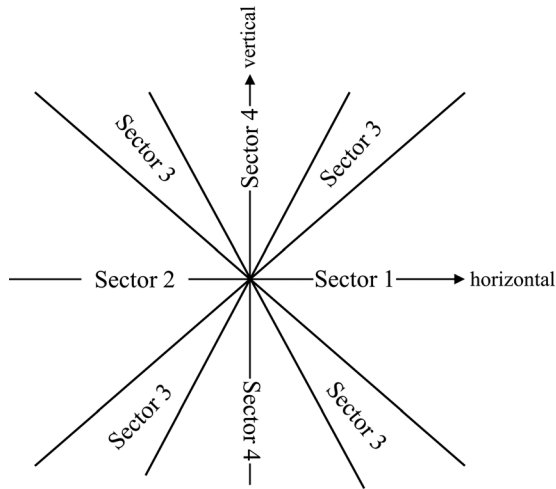


Fig. 3 Wind sectors

sectors depending on which turbine pairs have to be checked for wake cone overlap. Figure 3 shows the general distribution of the four sectors, and the exact definitions of the four sectors are provided below.

- Sector 1 contains all wind directions such that $j > i$ implies turbine j is downstream of turbine i .
- Sector 2 contains all wind directions such that $j < i$ implies turbine j is downstream of turbine i .
- Sector 3 contains wind directions where the ordering of the turbines along the horizontal axis does not imply any downstream or upstream relationships between turbine pairs.
- Sector 4 contains wind directions similar in nature to wind directions in Sector 3. The only difference is that wind directions in Sector 4 generate wake cones with one wake cone edge that does not cross the vertical axis.

Figure 4 shows an example of a wind direction in Sector 3 where turbine $i + 1$ is upstream of turbine i . The minimum angle threshold for a wind direction to be placed in Sector 3 or 4 depends on the diameter of the turbine disk, the wake expansion coefficient, and the size of the exclusion zone. The dotted lines in Fig. 4 are the boundaries of the interturbine exclusion zone which will be described in Sec. 2.2.

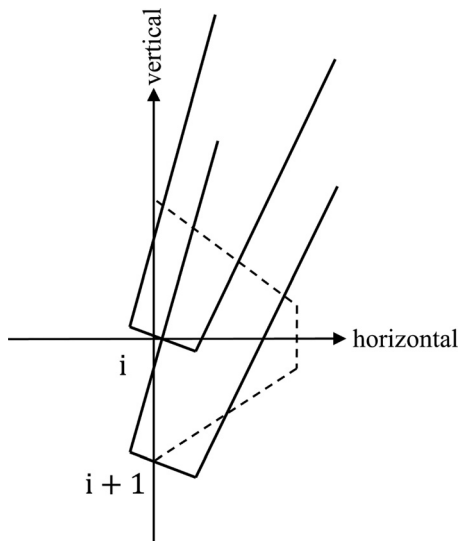


Fig. 4 Wake cone generated by wind direction in Sector 3

Wake cone overlap detection constraints for wind directions in Sectors 1 and 2 are straightforward—only conditions 1 and 2 need to be checked for turbine pairs (i, j) with indexes $i < j$ for wind directions in Sector 1, and $i > j$ for wind directions in Sector 2.

For wind directions in Sectors 3 and 4, the ordering of the turbines along the horizontal axis does not imply any upstream or downstream relationships between turbine pairs. However, there is no need to introduce new indicator variables and explicitly check for condition 3 since the downstream or upstream relationship between any pair of turbines for wind directions in Sectors 3 or 4 can be inferred from the wake cone membership test for the same pair of turbines in the horizontal wind direction (horizontal axis).

This principle is illustrated on the left side of Fig. 5 which highlights two possible Cases for turbine pair $(i, i + 1)$ and Sector 3 wind direction w_k .

In Case I, turbine $i + 1$ is located above the left edge of turbine i 's wake cone generated by the horizontal wind direction. This implies that turbine $i + 1$ is downstream of turbine i for w_k . In Case II, the fact that turbine $i + 1$ is located below the left edge of turbine i 's wake cone in the horizontal wind direction implies turbine $i + 1$ is upstream of turbine i for wind direction w_k .

For turbine pairs (i, j) , where $i > j$, and wind directions in Sector 3 or 4, one has to refer to the wake cone membership test for turbine pair (j, i) in the horizontal wind direction because the turbine pair (i, j) (where $i > j$) is not checked for wind directions in Sector 1.

This is illustrated on the right side of Fig. 5, which shows how the downstream/upstream relationship for turbine pair $(i, i - 1)$ can be inferred by checking turbine i 's position relative to the right edge of turbine $i - 1$'s wake cone in the horizontal direction.

In practical wind farm layout optimization problems, the minimum interturbine distance is many times larger than the diameter of the turbine disk, which means the above procedure is a reliable method for checking condition 3 for wind directions in Sectors 3 and 4.

Let $K_{3,4}^+$ and $K_{3,4}^-$ be the index set of wind directions in Sectors 3 and 4 which are in the upper and lower hemispheres, respectively. Table 1 summarizes the link between the binary wake cone membership detection variables $z_{1,ij}^+, z_{1,ij}^-$ from wind direction 1 (horizontal wind direction) and turbine downstream relationships (condition 3) for wind directions in Sectors 3 and 4.

For wind directions in Sector 3, both conditions 1 and 2 need to be checked for all turbine pairs (i, j) , where $i \neq j$. As for wind directions in Sector 4, the angle of the wind direction from the horizontal is large enough such that the generated wake cone has one edge which does not cross the vertical axis. This, together with the fact that the turbines are ordered along the horizontal axis, means it is only necessary to check either condition 1 or 2 depending on which hemisphere the wind direction belongs to. Table 2 summarizes the pairwise wake cone constraint tests that must be carried out for wind directions in each sector.

2.2 Proximity Constraints. The minimum interturbine distance in the proposed MILP formulation is expressed in terms of L^1 distance which creates a rhombus-shaped exclusion zone around each turbine. The reason for using L^1 distance is that the L^1 exclusion zone can be modeled using linear constraints and four binary indicator variables (1 for each edge) for each turbine pair i, j ($i < j$).

In the proposed formulation, no new binary variables are introduced. Instead, wake cone membership detection variables from the horizontal wind direction are used to create a truncated version of the L^1 exclusion zone shown in Fig. 6. The proposed exclusion zone is created using the constraints shown in Eq. (5).

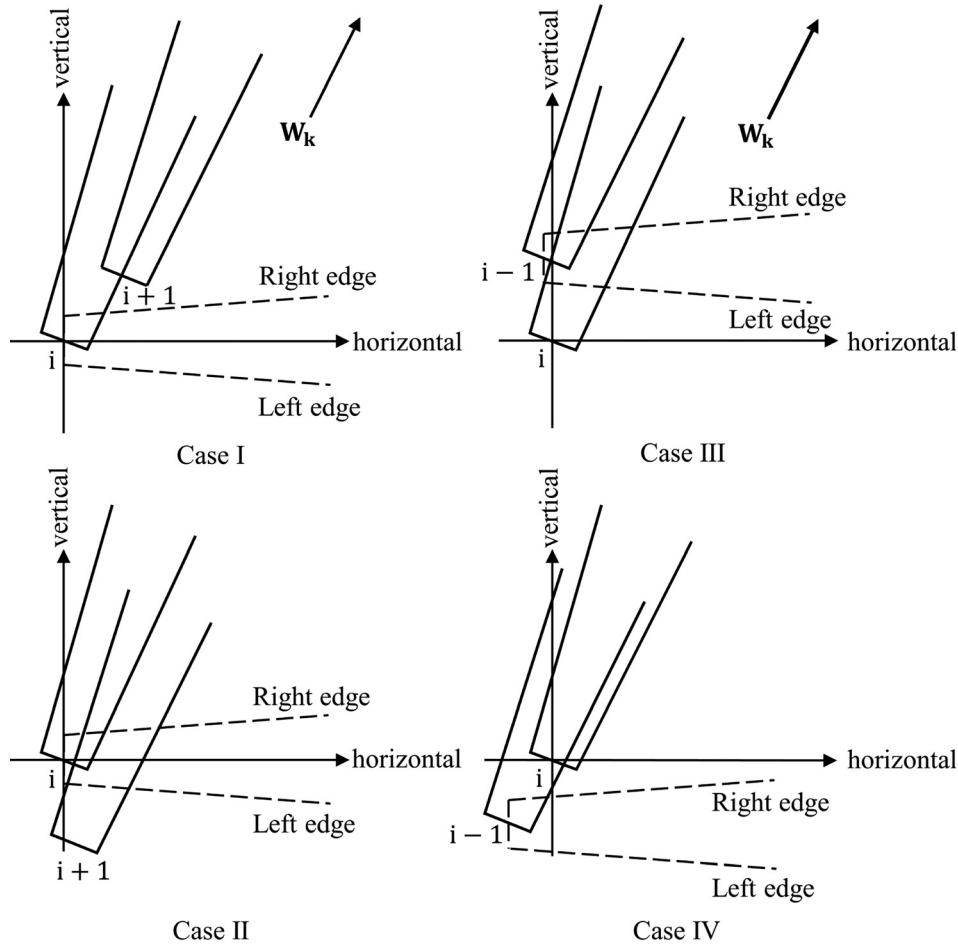


Fig. 5 Sector 3 upstream/downstream relationships

Table 1 Downstream test for wind directions in Sectors 3 and 4

$k \in K_{3,4}^+$ turbine pair (i, j)	$i < j$	Turbine j is downstream of i along direction k if $z_{1,ij}^l = 1$
	$i > j$	Turbine j is downstream of i along direction k if $z_{1,ji}^r = 1$
$k \in K_{3,4}^-$ turbine pair (i, j)	$i < j$	Turbine j is downstream of i along direction k if $z_{1,ij}^r = 1$
	$i > j$	Turbine j is downstream of i along direction k if $z_{1,ji}^l = 1$

Table 2 Pairwise wake cone overlap tests

Wind direction k	Check turbine pair	Check condition(s)
$\in K_1$	$i < j$	1 and 2
$\in K_2$	$i > j$	1 and 2
$\in K_3$	$i \neq j$	1 and 2
$\in K_4^+$	$i < j$	2
	$i > j$	1
$\in K_4^-$	$i < j$	1
	$i > j$	2

$$\begin{aligned}
 [\cos 45 \text{ deg}, \sin 45 \text{ deg}] \mathbf{x}_{ij} &\geq C - M_p z_{1,ij}^r \\
 [\cos 45 \text{ deg}, -\sin 45 \text{ deg}] \mathbf{x}_{ij} &\geq C - M_p z_{1,ij}^l \\
 \mathbf{w}_1^T \mathbf{x}_{ij} &\geq C' - M_p (2 - z_{1,ij}^r - z_{1,ij}^l) \\
 &\forall i, j \in T, \forall i < j
 \end{aligned} \tag{5}$$

The term M_p in Eq. (5) is a large constant that can be set to the minimum interturbine distance C plus the maximum straight-line distance in the wind farm. When turbine j in Fig. 6 is located above the right edge of turbine i 's horizontal wake cone, $z_{1,ij}^r = 0$

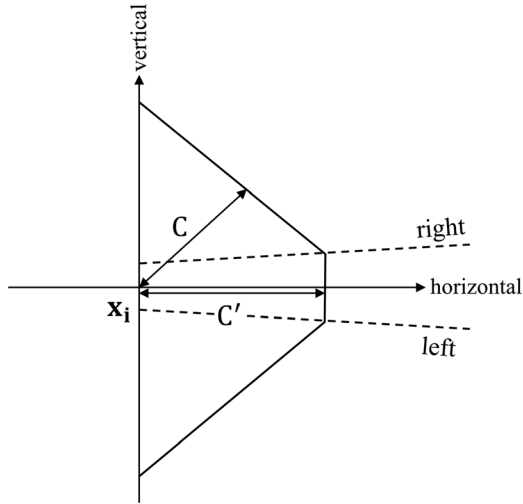


Fig. 6 Proposed exclusion zone

and $z_{1,ij}^l = 1$. This “switches off” the second and third constraints in Eq. (5) for turbine pair (i, j) since they are automatically satisfied. The M_p term in the first constraint disappears which “switches on” the constraint, ensuring that turbine j stays beyond the top slanted edge of turbine i 's exclusion zone.

The horizontal wake cone membership detection variables and M_p work together to switch constraints on or off in Eq. (5) depending on where turbine j is relative to turbine i . When turbine j is located below the left edge of turbine i 's horizontal wake cone ($z_{1,ij}^r = 1, z_{1,ij}^l = 0$), the second constraint is switched on while the other two are switched off. When turbine j is located inside turbine i 's wake cone ($z_{1,ij}^r = 1, z_{1,ij}^l = 1$), the third constraint is switched on while the other two are switched off.

The truncated exclusion zone has a “radius” of C' which can be easily calculated by finding the downstream distance at which a turbine's horizontal wake cone crosses the slanted edges of the L^1 exclusion zone with radius C . In most practical cases, C' will be larger than the minimum interturbine distance C , so any feasible solution satisfying Eq. (5) will satisfy the minimum interturbine distance requirement.

2.3 Objective Function. The proposed MILP formulation's objective is to minimize Eq. (6), where p_k is the probability of wind direction k , and ϕ_k is the highest pairwise power loss across all turbine pairs for wind direction k .

$$\sum_{k \in K} p_k \phi_k \quad (6)$$

Let $L_{k,ij}$ (Eq. (7)) denote the pairwise power loss for turbine pair (i, j) in wind direction k . If turbine j is not in turbine i 's wake

cone for direction k , then $L_{k,ij}$ is set to 0. If turbine j is deemed to be inside turbine i 's wake cone for direction k , $L_{k,ij}$ is given by $P(V_k) - P(V_{k,ij})$, where V_k is the average unobstructed wind speed in direction k , $V_{k,ij}$ is the wind speed in turbine i 's wake cone at turbine j 's downstream position along direction k , and $P(V)$ is turbine power generation as a function of incoming wind speed V . Note that $V_{k,ij}$ is evaluated with the assumption that turbine i 's incoming wind speed is V_k .

$$L_{k,ij} = \begin{cases} P(V_k) - P(V_{k,ij}) & \text{if } j \text{ is in } i\text{'s wake cone} \\ 0 & \text{otherwise} \end{cases} \quad (7)$$

$L_{k,ij}$ can be seen as a penalty function that discourages turbine pairs from overlapping. If overlaps occur, $L_{k,ij}$ uses power loss as a penalty to encourage further downstream placement of turbines. The overall objective is to minimize the probability-weighted sum of the highest $L_{k,ij}$ across all directions.

The objective function was chosen to be a reasonable substitute for more complicated and nonconvex power generation objective functions used in nonlinear formulations. The objective function used in this paper is similar in nature to previous MILP formulations that treat the power maximization problem as a geometric problem where the goal is to maximize some form of “distance” function between pairs of turbines. This approach is intuitive since one can maximize power generation by maximizing interturbine downstream distances along major wind directions. In this paper, the “distance” function is the pairwise power loss function which discourages wake cone overlaps. If overlaps do occur, the pairwise power loss function encourages further downstream placement of turbines along directions with high average wind speeds.

Furthermore, the chosen objective function can be easily approximated using linear splines, and the mini-max form greatly reduces the number of continuous variables compared to an objective function that sums up pairwise power loss for every turbine pair across all directions.

There are multiple ways of calculating $V_{k,ij}$ in the literature. In this paper, $V_{k,ij}$ is calculated using: $V_{k,ij} = (1 - dv_{k,ij})V_k$, where $dv_{k,ij}$ is the fractional wind speed deficit experienced by turbine j due to turbine i for direction k . According to Lackner and Elkinton [18], $dv_{k,ij}$ can be calculated using Eq. (8), where $C_t(V)$ is the turbine's thrust coefficient as a function of incoming wind speed V , D_0 is the diameter of the turbine disk, and $D(d_{k,ij})$ is the diameter of the wake cone generated by turbine i at a downstream distance of $d_{k,ij}$ (Eq. (1)).

$$dv_{k,ij} = \frac{(1 - \sqrt{1 - C_t(V_k)})D_0^2}{D(d_{k,ij})^2} \quad (8)$$

The left side of Fig. 7 illustrates how the nonzero part of $L_{k,ij}$ is a convex, decreasing function with respect to downstream position of turbine j . This means the nonzero part of $L_{k,ij}$ can be approximated using piecewise linear splines as shown in the right

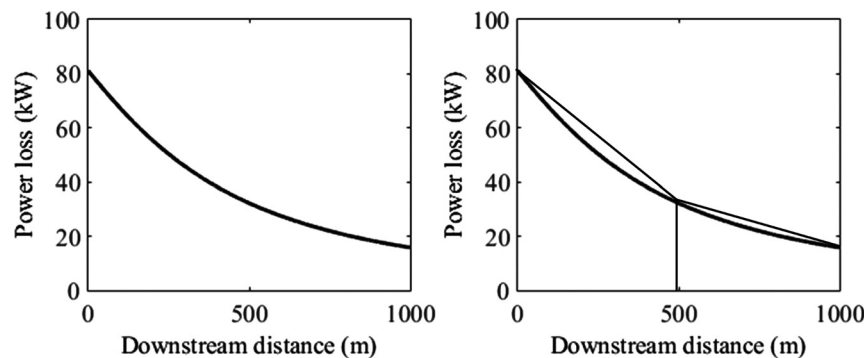


Fig. 7 Power loss curve and trapezoid approximation

side of Fig. 7. Let N_a denote the number of linear splines used in the approximation, then the piecewise linear approximation of the curve can be easily obtained by finding the best N_a -trapezoid estimation of the area under the curve over the longest possible downstream distance in direction k .

For each wind direction k , let $\alpha_{k,1}, \dots, \alpha_{k,N_a}$ and $\beta_{k,1}, \dots, \beta_{k,N_a}$ denote the gradients and intercepts, respectively, of the N_a linear splines that form the linear approximation of the nonzero part of $L_{k,ij}$ with respect to downstream distance. The objective can then be expressed in mini-max form shown in Eq. (9).

The term M_{obj} is a large constant that can be set to the maximum possible value of $\alpha_{k,s}\mathbf{x}_{ij}^T\mathbf{w}_k + \beta_{k,s}$ across all k, s , and feasible \mathbf{x}_{ij} . M_{obj} and wake cone membership indicator variables work together in Eq. (9) to implement the binary nature of $L_{k,ij}$ by switching constraints on or off depending on whether turbine j is in turbine i 's wake cone for wind direction k . As mentioned previously, wake cone indicator variables for the horizontal wind direction ($z_{1,ij}^r, z_{1,ij}^l$) are used to determine upstream/downstream relationships for wind directions in Sectors 3 and 4.

$$\begin{aligned} & \min \sum_{k \in K} \phi_k \\ & \text{subject to:} \\ & \frac{\phi_k}{p_k} \geq \alpha_{k,s}\mathbf{x}_{ij}^T\mathbf{w}_k + \beta_{k,s} - M_{obj}(2 - z_{k,ij}^r - z_{k,ij}^l) \\ & \quad \forall k \in K_1 \cup K_2, \forall s \in \{1, \dots, N_a\}, \forall i, j \in T \\ & \quad \quad i < j \text{ if } k \in K_1, \quad i > j \text{ if } k \in K_2 \\ & \frac{\phi_k}{p_k} \geq \alpha_{k,s}\mathbf{x}_{ij}^T\mathbf{w}_k + \beta_{k,s} - M_{obj}(3 - z_{k,ij}^r - z_{k,ij}^l - z_{1,ij}^l) \\ & \quad \forall k \in K_3^+ \cup K_3^-, \forall s \in \{1, \dots, N_a\}, \forall i, j \in T \\ & \quad \quad i < j \text{ if } k \in K_3^+, \quad i > j \text{ if } k \in K_3^- \\ & \frac{\phi_k}{p_k} \geq \alpha_{k,s}\mathbf{x}_{ij}^T\mathbf{w}_k + \beta_{k,s} - M_{obj}(3 - z_{k,ij}^r - z_{k,ij}^l - z_{1,ij}^r) \\ & \quad \forall k \in K_3^+ \cup K_3^-, \forall s \in \{1, \dots, N_a\}, \forall i, j \in T \\ & \quad \quad i > j \text{ if } k \in K_3^+, \quad i < j \text{ if } k \in K_3^- \\ & \frac{\phi_k}{p_k} \geq \alpha_{k,s}\mathbf{x}_{ij}^T\mathbf{w}_k + \beta_{k,s} - M_{obj}(2 - z_{k,ij}^l - z_{1,ij}^l) \\ & \quad \forall k \in K_4^+ \cup K_4^-, \forall s \in \{1, \dots, N_a\}, \forall i, j \in T \\ & \quad \quad i < j \text{ if } k \in K_4^+, \quad i > j \text{ if } k \in K_4^- \\ & \frac{\phi_k}{p_k} \geq \alpha_{k,s}\mathbf{x}_{ij}^T\mathbf{w}_k + \beta_{k,s} - M_{obj}(2 - z_{k,ij}^r - z_{1,ij}^r) \\ & \quad \forall k \in K_4^+ \cup K_4^-, \forall s \in \{1, \dots, N_a\}, \forall i, j \in T \\ & \quad \quad i > j \text{ if } k \in K_4^+, \quad i < j \text{ if } k \in K_4^- \\ & \phi_k \geq 0 \quad \forall k \in K \end{aligned} \quad (9)$$

2.4 Final MILP Formulation. In most wind farm layout problems, wind directions form opposing pairs, i.e., for every direction \mathbf{w} there exists an opposite direction $-\mathbf{w}$. In such cases,

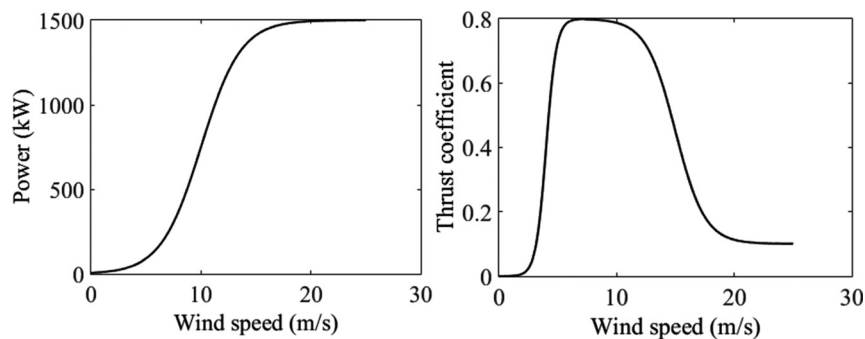


Fig. 8 Turbine power and thrust coefficient curves

Table 3 Turbine specifications

Parameter	Value
Diameter, D_0	80 m
Wake expansion coefficient, κ	0.075
Minimum interturbine distance, C	320 m
Rated power	1500 kW

the problem size can be greatly reduced since wake cone membership for two opposing directions is identical. For example, if turbine j is in turbine i 's wake cone for direction \mathbf{w} , then this implies turbine i is in turbine j 's wake cone for direction $-\mathbf{w}$.

Let K_0 denote the initial index set of wind directions. If the wind directions in K_0 form opposing pairs, then for every opposing pair in K_0 , arbitrarily choose one direction and add its index to K . If K_0 does not have opposing wind directions, set $K = K_0$.

The probability of occurrence of wind direction $k \in K$ is set to $p_{k \in K_0} + p_{k^* \in K_0}$, where k^* is the index of the opposing direction to k . In addition, each gradient ($\alpha_{k,l}$) and intercept ($\beta_{k,l}$) of the piecewise linear approximation of the pairwise power loss curve for direction $k \in K$ is set to $\alpha_{k \in K_0,l} + \alpha_{k^* \in K_0,l}$ and $\beta_{k \in K_0,l} + \beta_{k^* \in K_0,l}$, respectively.

For brevity sake, let S_{wc} denote the feasible space defined by the wake cone membership test constraints for Sectors 1, 2, 3, and 4. Also, let S_{prox} and S_{bound} denote the feasible spaces defined by the proximity constraints (Eq. (5)) and upper bound constraints (Eq. (9)), respectively, and let F be a polyhedral set representing the boundaries of the wind farm. The full MILP formulation is given below in the following equation:

$$\begin{aligned} & \min \sum_{k \in K} \phi_k \\ & \mathbf{Y} = [\mathbf{U}, \mathbf{X}, \mathbf{Z}]^T \\ & \text{subject to:} \\ & x_{i,hor} < x_{j,hor} \quad \forall i, j \in T, \quad \forall i < j \\ & [\mathbf{X}, \mathbf{Z}] \in S_{wc} \\ & [\mathbf{X}, \mathbf{Z}] \in S_{prox} \\ & \mathbf{Y} \in S_{bound} \\ & \mathbf{X} \in F \end{aligned} \quad (10)$$

All decision variables in MILP formulation are placed in the vector $\mathbf{Y} = [\mathbf{U}, \mathbf{X}, \mathbf{Z}]^T$. $\mathbf{U} \in \mathbb{R}^{|K|}$ is the vector of upper bound variables $\phi_{k \in K}$; $\mathbf{X} \in \mathbb{R}^{2|T|}$ is the vector of turbine locations with components $[\mathbf{x}_1, \dots, \mathbf{x}_{|T|}]^T$, and $\mathbf{Z} \in \{0, 1\}^{n_z}$ is the binary vector of wake cone membership detection variables with dimension $n_z = (|K_1| + |K_2| + 2|K_3| + |K_4|)[|T|(|T| - 1)]$.

3 Comparison to Grid-Based Approach

The proposed MILP was compared to a grid-based MILP formulation (GRID-MILP) adapted from Ref. [6]. The overall structure of the formulation used in Ref. [6] was kept the same, but the wake model and power curve were replaced with the ones used in this paper. The objective function in Ref. [6] was also changed

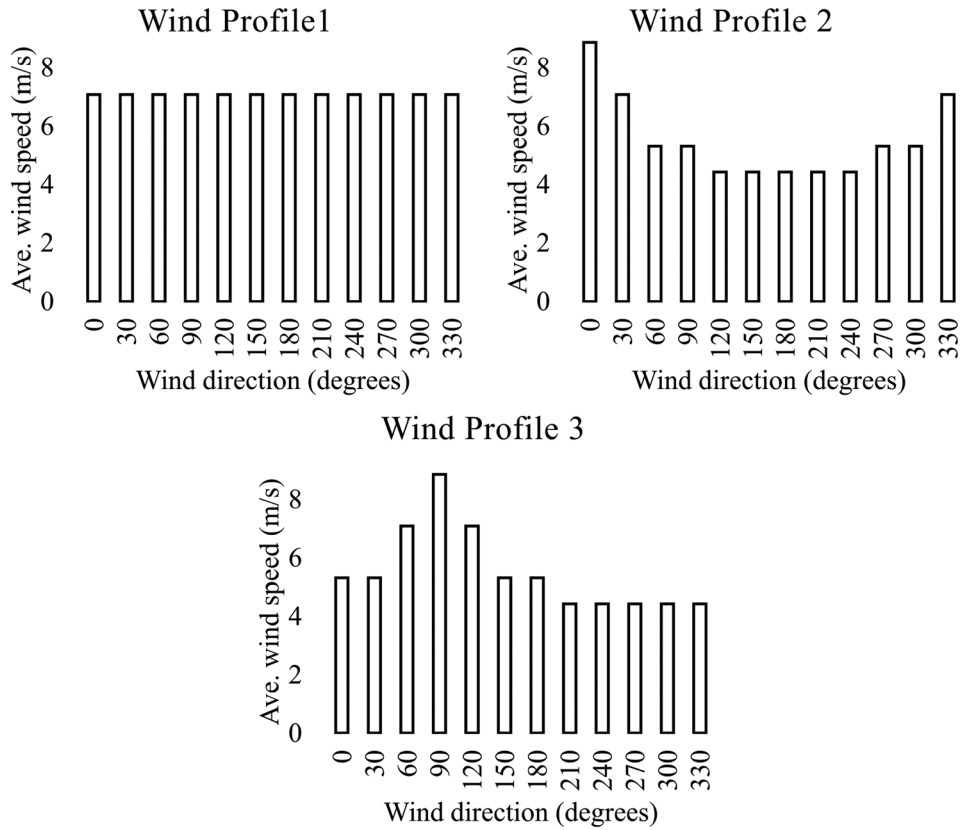


Fig. 9 Wind speed profiles

Table 4 Wind farm dimensions

Label	Wind farm dimension
SQ	960 × 960 m
RT	640 × 1920 m

from minimizing total pairwise wind speed loss to minimizing the probability-weighted sum of pairwise power loss defined in Eq. (7). In addition, GRID-MILP uses the actual pairwise power loss function instead of a linear-spline approximation, and GRID-MILP accounts for partial wake cone overlap in the way described in Refs. [20] and [28] when calculating fractional wind speed deficit $dv_{k,ij}$ (Eq. (8)). The GRID-MILP formulation used in the comparison is shown in Eq. (11).

In Eq. (11), J is the index set of feasible turbine locations labeled from 1 to N . x_i is a binary decision variable that is 1 if a turbine is placed on point i . The points are spread regularly throughout the wind farm with spacing equal to the minimum interturbine distance C . The decision variable y_{ij} takes the value of 1 if there are turbines located on points i and j . The coefficient a_{ij} in the objective function is the probability-weighted sum of the pairwise power loss experienced by turbine j due to turbine i and vice versa across all wind directions k (Eq. (12)).

$$\begin{aligned} \min \quad & \sum_{i,j \in J, i < j} a_{ij} y_{ij} \\ \text{subject to:} \quad & \sum_{i=1}^N x_i = |T| \end{aligned} \quad (11)$$

$$\begin{aligned} y_{ij} &\geq x_i + x_j - 1 \quad \forall i, j \in J, i < j \\ x_i &\in \{0, 1\} \quad \forall i = 1, \dots, N \\ y_{ij} &\geq 0 \quad \forall i, j \in J, i < j \end{aligned}$$

GRID-MILP and the proposed MILP offer two different mathematical programming approaches for discrete, linear, wind farm layout optimization. GRID-MILP uses continuous models for wake cone overlap and power generation, but discretizes the feasible space for turbine placement. The proposed MILP formulation

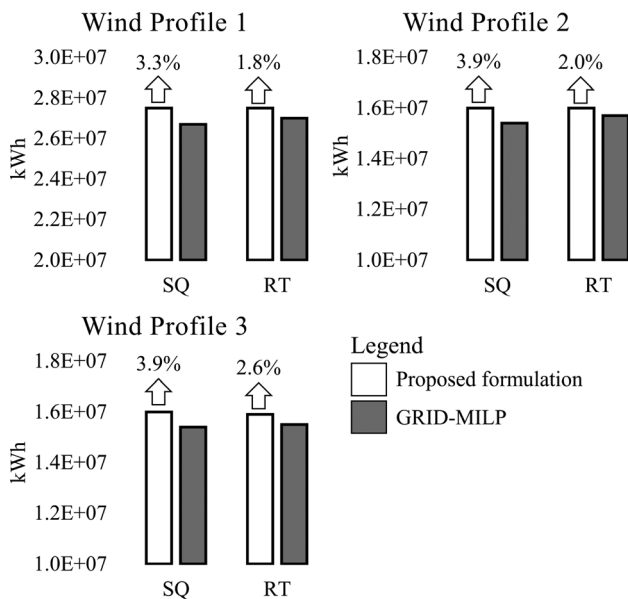


Fig. 10 AEP comparison

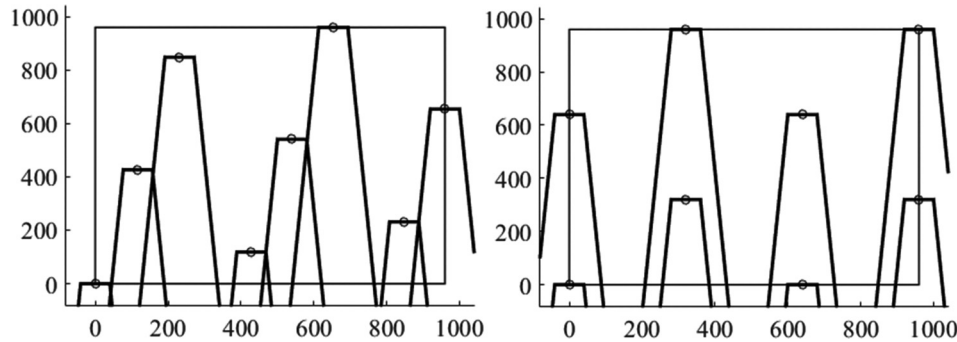


Fig. 11 Wake cones generated along the 270 deg direction in the square wind farm

discretizes wake cone overlap and uses a linear-spline approximation of pairwise power loss, but the feasible space for turbine placement is continuous.

$$a_{ij} = \sum_{k \in K} p_k(L_{k,ij} + L_{k,ji}) \quad (12)$$

The two formulations were compared over different wind profiles, wind farm sizes and shapes. The number of turbines was fixed at 8 in all comparison scenarios. The turbine specifications, and power and thrust curves are shown in Table 3 and Fig. 8, respectively. The turbine power curve was based on the power curve of the 5 MW wind turbine model created by the National Renewable Energy Laboratory [29].

Three wind profiles were used, with each profile having 12 equally spaced out wind directions with equal probability of occurring. The average wind speeds of each wind profile are shown in Fig. 9. Note that wind profile 3 is the same as rotating wind profile 2 90 deg counterclockwise.

Each wind profile was paired with two wind farms labeled SQ and RT with dimensions shown in Table 4, bringing the total number of comparison scenarios to six. In all scenarios, the bottom left corner of the wind farm was set as the origin, and the 0 deg wind direction was set as the positive horizontal direction.

The two formulations were compared based on their optimal solutions' annual energy production (AEP) defined in Ref. [28]. AEP represents the expected power generated by the wind farm over a year assuming some wind speed probability distribution for each wind direction. In this case, the Weibull distribution was used for every direction, with all scale parameters set to 2, and shape parameter for each direction chosen such that the average wind speeds match the average wind speeds shown in Fig. 9. The comparison results are shown in Fig. 10.

The wind farms used in the comparison were relatively constrained in terms of available space per turbine, so the proposed formulation's results shown in Fig. 10 represent a decent improvement in expected annual power generation over the layouts generated by GRID-MILP. In addition, the variation in power generation for both formulations was the same. The mean to standard deviation ratio for annual power generation was around 0.92 for both formulations under wind profile 1, and around 0.68 for both formulations under wind profiles 2 and 3.

One can better understand the advantage of unrestricted turbine placement by referring to Fig. 11 which shows the wake cones of the turbine layouts generated by the two approaches for one of the comparison scenarios. When turbine placement is restricted to a grid, GRID-MILP has limited options in finding overlap-free layouts, but when turbine placement is unrestricted, the proposed formulation will be able to find an overlap-free layout if it exists.

4 Conclusion

This paper presented a novel MILP formulation for unrestricted wind farm layout optimization. Linearity of the formulation was

maintained by treating wake cone overlap as a binary outcome and using a linear approximation of the pairwise power loss function. Despite the simplifications, the expansion of feasible space for turbine placement led to better solutions compared to a modified version of the grid-based MILP formulation from Ref. [6].

A large amount of effort was spent on making the proposed formulation as small as possible in terms of the number of binary variables. However, despite these efforts, the formulation still struggles to provide optimal solutions for larger wind farms with more than 20 turbines, or more complicated wind profiles with more than 12 directions.

One reason why the proposed formulation performs poorly for large problems is that the formulation relies heavily on "big-M" constraints to model the binary objective and wake cone overlaps. The linear relaxations of these big-M formulations provide poor bounds for the mixed integer optimal value (even when the big-M constants are set properly), which leads to slow branch and bound performance for large problems. Coming up with an alternative formulation without relying on big-M constraints is no trivial task, but such a formulation might make it easier to obtain high quality bounds for the branch and bound algorithm.

Another way of handling large problems is to use global search heuristics such as a GA to find a good, but not necessarily optimal, solution for the proposed MILP formulation. It might also be possible to break up a large problem into smaller parts by grouping turbines together, and then solving the smaller parts to optimality before coming up with some heuristic for combining the solutions together.

Regardless of whichever heuristic is used, it is unlikely to come with any global optimality guarantees. Nonetheless, the proposed formulation has shown that it can provide better solutions than grid-based formulations, especially when the grid resolution is low, so there is a value in extending the concepts and ideas introduced in this paper to much larger wind farms where the improvement in power generation due to intelligent turbine layout could be even greater.

Nomenclature

- C = minimum interturbine distance
- $C_t(V)$ = turbine thrust coefficient at incoming wind speed V
- $dv_{k,ij}$ = fractional wind speed deficit experienced by turbine j due to turbine i for wind direction k
- D_0 = turbine diameter
- $D(d)$ = wake cone diameter at downstream distance d
- K = index set of wind directions
- K_m^+ = index set of wind directions in sector m that are in the upper hemisphere [0 deg, 180 deg)
- K_m^- = index set of wind directions in sector m that are in the lower hemisphere [180 deg, 360 deg)
- $L_{k,ij}$ = pairwise power loss for turbine pair (i, j) in direction k
- M_{obj} = big-M constant in lower bound constraints in mini-max objective
- M_p = big-M constant in proximity constraints

M_w = big-M constant in wake cone membership detection constraints
 N_a = number of linear splines used in the piecewise linear approximation of the pairwise power loss curve
 $P(V)$ = turbine power generated with incoming wind speed V
 p_k = probability of wind direction k
 T = index set of turbines
 V_k = average unobstructed wind speed in direction k
 $V_{k,ij}$ = wind speed in turbine i 's wake cone along wind direction k at turbine j 's downstream position
 \mathbf{w}_k = unit vector representing wind direction k
 \mathbf{w}_k^r = right orthogonal unit vector to \mathbf{w}_k
 \mathbf{w}_k^l = left orthogonal unit vector to \mathbf{w}_k
 \mathbf{x}_i = vector representing the location of turbine i
 \mathbf{x}_i^r = position of right edge of turbine i 's disk
 \mathbf{x}_i^l = position of left edge of turbine i 's disk
 \mathbf{x}_{ij} = vector from turbine i to turbine j
 $x_{i,\text{hor}}$ = horizontal coordinate of turbine i
 $z_{k,ij}^f$ = condition 1 indicator variable for wind direction k and turbine pair (i, j)
 $z_{k,ij}^l$ = condition 2 indicator variable for wind direction k and turbine pair (i, j)

Greek Symbols

$\alpha_{k,l}$ = gradient of the l th linear spline in the piecewise linear approximation of the pairwise power loss curve for wind direction k
 $\beta_{k,l}$ = intercept of the l th linear spline in the piecewise linear approximation of the pairwise power loss curve for wind direction k
 κ = wake cone expansion coefficient
 ϕ_k = highest pairwise power loss across all turbine pairs for wind direction k

References

- [1] Pineda, I., Azau, S., Moccia, J., and Wilkes, J., 2014, "Wind in Power, 2013 European Statistics," The European Wind Energy Association, Last accessed Jan. 8, 2015, http://www.ewea.org/fileadmin/files/library/publications/statistics/EWEA_Annual_Statistics_2013.pdf
- [2] Wiser, R., and Bolinger, M., 2012, "2012 Wind Technologies Market Report," United States Department of Energy, Last accessed Jan. 8, 2015, https://www1.eere.energy.gov/wind/pdfs/2012_wind_technologies_market_report.pdf
- [3] González, J. S., Payán, M. B., Santos, J. M. R., and González-Longatt, F., 2014, "A Review and Recent Developments in the Optimal Wind-Turbine Micro-Siting Problem," *Renewable Sustainable Energy Rev.*, **30**, pp. 133–144.
- [4] Herbert-Acero, J. F., Probst, O., Réthoré, P.-E., Larsen, G. C., and Castillo-Villar, K. K., 2014, "A Review of Methodological Approaches for the Design and Optimization of Wind Farms," *Energies*, **7**(11), pp. 6930–7016.
- [5] Zhang, P. Y., Romero, D. A., Beck, J. C., and Amon, C. H., 2014, "Solving Wind Farm Layout Optimization With Mixed Integer Programs and Constraint Programming," *EURO J. Comput. Optim.*, **2**(3), pp. 195–219.
- [6] Turner, S. D. O., Romero, D. A., Zhang, P. Y., Amon, C. H., and Chan, T. C. Y., 2014, "A New Mathematical Programming Approach to Optimize Wind Farm Layouts," *Renewable Energy*, **63**, pp. 674–680.
- [7] Bertsimas, D., and Weismantel, R., 2005, *Optimization Over Integers*, Dynamic Ideas, Belmont, MA.
- [8] Mosetti, G., Poloni, C., and Diviacco, B., 1994, "Optimization of Wind Turbine Positioning in Large Windfarms by Means of a Genetic Algorithm," *J. Wind Eng. Ind. Aerodyn.*, **51**(1), pp. 105–116.
- [9] Grady, S. A., Hussaini, M. Y., and Abdullah, M. M., 2005, "Placement of Wind Turbines Using Genetic Algorithms," *Renewable Energy*, **30**(2), pp. 259–270.
- [10] Salcedo-Sanz, S., Gallo-Marazuela, D., Pastor-Sánchez, A., Carro-Calvo, L., Portilla-Figueras, A., and Prieto, L., 2013, "Evolutionary Computation Approaches for Real Offshore Wind Farm Layout: A Case Study in Northern Europe," *Expert Syst. Appl.*, **40**(16), pp. 6292–6297.
- [11] Chen, L., and MacDonald, E., 2012, "Considering Landowner Participation in Wind Farm Layout Optimization," *ASME J. Mech. Des.*, **134**(8), p. 084506.
- [12] Chen, K., Song, M. X., He, Z. Y., and Zhang, X., 2013, "Wind Turbine Positioning Optimization of Wind Farm Using Greedy Algorithm," *J. Renewable Sustainable Energy*, **5**, p. 023128.
- [13] Dobrić, G., and Durisić, Z., 2014, "Double-Stage Genetic Algorithm for Wind Farm Layout Optimization on Complex Terrains," *J. Renewable Sustainable Energy*, **6**, p. 033127.
- [14] Song, M., Chen, K., Zhang, X., and Wang, J., 2015, "The Lazy Greedy Algorithm for Power Optimization of Wind Turbine Positioning on Complex Terrain," *Energy*, **80**, pp. 567–574.
- [15] Kwong, W. Y., Zhang, P. Y., Romero, D., Moran, J., Morgenroth, M., and Amon, C., 2014, "Multi-Objective Wind Farm Layout Optimization Considering Energy Generation and Noise Propagation With NSGA-II," *ASME J. Mech. Des.*, **136**(9), p. 091010.
- [16] Crespo, A., Hernández, J., and Frandsen, S., 1999, "Survey of Modelling Methods for Wind Turbine Wakes and Wind Farms," *Wind Energy*, **2**(1), pp. 1–24.
- [17] Frandsen, S., Barthelme, R., Pryor, S., Rathmann, O., Larsen, S., Højstrup, J., and Thøgersen, M., 2006, "Analytical Modeling of Wind Speed Deficit in Large Offshore Wind Farms," *Wind Energy*, **9**(1–2), pp. 39–53.
- [18] Lackner, M. A., and Elkinton, C. N., 2007, "An Analytical Framework for Offshore Wind Farm Layout Optimization," *Wind Eng.*, **31**(1), pp. 17–31.
- [19] Kusiak, A., and Song, Z., 2010, "Design of Wind Farm Layout for Maximum Wind Energy Capture," *Renewable Energy*, **35**(3), pp. 685–694.
- [20] Lu, S., and Kim, H. M., 2014, "Wind Farm Layout Design Optimization Through Multi-Scenario Decomposition With Complementarity Constraints," *Eng. Optim.*, **46**(12), pp. 1669–1693.
- [21] Du Pont, B. L., and Cagan, J., 2012, "An Extended Pattern Search Approach to Wind Farm Layout Optimization," *ASME J. Mech. Des.*, **134**(8), p. 081002.
- [22] Eroğlu, Y., and Seçkiner, S. U., 2012, "Design of Wind Farm Layout Using Ant Colony Algorithm," *Renewable Energy*, **44**, pp. 53–62.
- [23] Chowdhury, S., Zhang, J., Messac, A., and Castillo, L., 2013, "Optimizing the Arrangement and the Selection of Turbines for Wind Farms Subject to Varying Wind Conditions," *Renewable Energy*, **52**, pp. 273–282.
- [24] Réthoré, P.-E., Fuglsang, P., Larsen, G. C., Buhl, T., Larsen, T. J., and Madsen, H. A., 2014, "TOPFARM: Multi-Fidelity Optimization of Wind Farms," *Wind Energy*, **17**(12), pp. 1797–1816.
- [25] Wagner, M., Day, J., and Neumann, F., 2013, "A Fast and Effective Local Search Algorithm for Optimizing the Placement of Wind Turbines," *Renewable Energy*, **51**, pp. 64–70.
- [26] Park, J., and Law, K. H., 2015, "Layout Optimization for Maximizing Wind Farm Power Production Using Sequential Convex Programming," *Appl. Energy*, **151**, pp. 320–334.
- [27] Long, H., and Zhang, Z., 2015, "A Two-Echelon Wind Farm Layout Planning Model," *IEEE Trans. Sustainable Energy*, **6**(3), pp. 863–871.
- [28] Pérez, B., Mínguez, R., and Guanache, R., 2013, "Offshore Wind Farm Layout Optimization Using Mathematical Programming Techniques," *Renewable Energy*, **53**, pp. 389–399.
- [29] Jonkman, J., Butterfield, S., Musial, W., and Scott, G., 2009, "Definition of a 5-MW Reference Wind Turbine for Offshore System Development," National Renewable Energy Laboratory, *Technical Report No. NREL/TP-500-38060*.